RESEARCH ARTICLE

Vertical distribution of soil salinity and nutrients in the oasis within the headstream area of the Tarim river, southern Xinjiang, China, and predictive modeling based on critical layers

Runze Wang[1, 2, 3, 4, 5], Fei Zhang[2], Yangxiaoxiao Shi[1, 3, 4, 5], Jinhu Zhi[1, 3, 4, 5, *]

[1]College of Agriculture, Tarim University, Alar, Xinjiang, China. [2]Observation and Research Station of Soil and Water Process and Ecological Security of Oasis in the Headstream Area of the Tarim River, MNR, Urumqi, Xinjiang, China. [3]Key Laboratory of Genetic Improvement and Efficient Production for Specialty Crops in Arid Southern Xinjiang of Xinjiang Corps, Alar, Xinjiang, China. [4]Collaborative Innovation Center of Eco-Agriculture around Tarim, Alar, Xinjiang, China. [5]The Research Center of Oasis Agricultural Resources and Environment in Southern Xinjiang, Tarim University, Alar, Xinjiang, China.

Received: March 20, 2026; **accepted:** April 26, 2026.

Salinized soils are prevalent worldwide, constituting a major constraint on agricultural productivity. Intensive fertilization has been widely adopted to enhance productivity in these soils. However, the vertical distribution of salt and nutrients from surface to deeper soil layers remains insufficiently characterized. This knowledge gap is particularly pronounced in saline agricultural systems, where root systems and subsurface drainage pipes extend to depths of up to two meters. This research collected a total of 106 soil samples spanning 0 – 200 cm from cotton fields and jujube orchards to analyze salt and nutrient contents and correlations. A random forest model was employed to predict their contents in deeper layers or across the entire profile. The results showed that local soil salinity ranged from 0.53 – 2.43 g/kg and was concentrated mainly in the 0 – 40 cm soil layer, where values commonly exceeded 0.5%. Soil salinity was primarily driven by Ca^{2+}, Mg^{2+}, SO_4^{2-}, and K^+. The most abundant nutrient was available potassium (K) followed by mineral nitrogen (N), both decreasing gradually across the 0 – 200 cm depth range. Available phosphorus (P) exhibited the least abundant and nearly undetectable at 200 cm depth in both cotton fields and jujube orchards. Consequently, positive correlations with salinity were only observed for available K and mineral N. Regarding both correlation strength and statistical significance, these correlations were stronger in cotton fields than in orchards, and stronger in topsoil than in subsoil. Random forest model indicated that the 0 – 40 cm layer was critical for salinity variation, exhibiting correlations of 0.9226 and 0.9604 with deeper layer and whole profile salinity, respectively. The results suggested potential for streamlining fieldwork by assessing salinity at 0 – 40 cm to infer salinization across the entire 0 – 200 cm profile. By contrast, the model performed less well for nutrients, which reflected the fact that salt distribution across depths responded strongly to irrigation and evaporation, whereas nutrients exhibited lower mobility. This study significantly advanced the understanding of deep-profile (0 – 200 cm) salinity-nutrient dynamics in arid agroecosystems, while also providing a cost-effective predictive modeling approach that enabled reliable inference of total profile salinization from surface soil data alone.

Keywords: soil salinity; soil nutrient; vertical distribution; random forest.

[*]**Corresponding author:** Jinhu Zhi, College of Agriculture, Tarim University, Alar, Xinjiang 843300, China. Email: zjhzky@163.com.

Introduction

Land scarcity and declining farmland quality compelled China to reclaim marginally to moderately saline-sodic soils for agriculture during the 1950s to address food insecurity. The country holds more than 100 million hectares of such soil, mainly in the northwest, northeast, and coastal zones, while Xinjiang Uygur Autonomous Region contains 36.8% of the national total [1]. Outside deserts and mountains areas, saline-alkali land dominates the landscape, exceeding 90% of the surface in southern Xinjiang [2]. High salinity threatens plants and soil microorganisms and is the principal driver of low productivity. It also degrades physicochemical properties, reducing water retention, increasing soil compaction and stickiness, and slowing nutrient release, thereby constraining agriculture [3]. Xinjiang's geology includes ancient marine sediments and Tertiary saline deposits, giving the region a higher baseline salinity than elsewhere [4]. Additionally, as the area is in an extremely arid region with annual evaporation exceeding 2,000 mm reported by local meteorological bureau, capillary rise transports salts to the surface, where they crystallize [5]. To cope with aridity, farmers apply dissolved fertilizer through mulched drip irrigation, maintaining soil moisture just above the crop wilting point and improving water use efficiency. However, water loss *via* transpiration leaves salt behind, inducing secondary salinization. Seasonal flood irrigation in spring and winter leaches salt through drainage pipes, temporarily lowering salinity. Yet, this practice simultaneously strips nutrients and reduces microbial diversity, causing a sharp decline in soil fertility [6].

Salinized soil is typically characterized by an imbalance between soluble salts and plant-available nutrients. Hui *et al*. profiled the 0 – 100 cm layer near Qarhan Salt Lake and found that salinity correlated negatively with nutrient content. Cl^-, Na^+, K^+, and SO_4^{2-} constrained nutrient and salt concentrations more strongly than Ca^{2+}, Mg^{2+}, CO_3^{2-}, and HCO_3^-. The effect was the strongest in the surface 0 – 20 cm, where salt accumulation altered the microbial pools of nitrogen (N), phosphorus (P), and carbon (C) [7]. A comparable study in Hotan, Xinjiang, China also reported inverse salinity-nutrient relationships associated with anthropogenic disturbance. Fertilization raised organic matter and N, P, and potassium (K) contents, while groundwater pumping and leaching lowered salinity in cultivated compared to uncultivated land [8]. Conversely, another work documented a positive correlation that fertilization increased nutrient status, yet simultaneously intensified salinization, reduced crop biomass by 25 – 30% and disrupted ionic balance [9]. However, these surveys were restricted to small and shallow plots. Less information exists on the vertical distribution of salts and nutrients below 1 meter. This gap is critical, because local cash crops, jujube and cotton, are drought-tolerant perennials whose active roots penetrate 0.6 to over 1.0 m [10, 11], and subsurface pipe drainage pipes can be installed as deep as 1.8 m [12]. Growing plants and fluctuating water levels drive substance exchange across the whole profile, yet few studies have sampled below the general plough layer. This limitation hinders integrated management of salinity and fertility in arid-zone agriculture. Sodium concentration and the permeability index display significant spatial correlation. Under drip irrigation, salt is leached downward, whereas flood irrigation redistributes them upward [13]. During successive wetting-drying cycles, these opposing fluxes force soil solutions to oscillate, generating statistical dependence among salinity values at different depths. Guan *et al*. reported that irrigation produced an abrupt moisture increase in the 30 – 70 cm layer beneath cotton. Salts first migrated below 70 cm, then rose above 30 cm as infiltration declined and evaporation predominated, yielding a negative salinity correlation between surface and deeper layer [14]. Nutrients are transported with water, K and N were relatively mobile and declined with depth, whereas P was immobilized, and its lability was further restrained by metal ions. As a result, linear correlations showed weak effects at deeper layers [15]. Machine-learning models have recently been used to predict vertical distributions of organic carbon and salinity, confirming that the surface layer functions as a reservoir that strongly influences substance contents in deeper [16, 17]. However, the potential of such models to predict profile-scale salinity and nutrients distribution remains largely untested, despite their practical value for strata where sampling is difficult.

This study collected soil samples from the 0 – 200 cm layer to determine salt and nutrient contents and used machine-learning models to predict their vertical distribution. By characterizing the vertical distribution of salts and nutrients in saline soils collected from cotton fields and jujube orchards, revealing potential correlation between salts and nutrients in various soil layers, and predicting the salts and nutrients content through proposed random forest model to benefit the estimation of the degree of salinity and soil fertility in deep layer, this research filled the blank of local soil salinity and nutrient situation and enriched the global saline alkali soil database. The proposed model was potentially able to build a bridge between various soil layers and guide effective agricultural activity.

Materials and methods

Study area

This study was conducted in an oasis within the headstream area of the Tarim River in Xinjiang Uygur Autonomous Region, China, located in the northern edge of the Taklimakan Desert and south of Tianshan Mountain with the geographic coordinates of 40.42°N – 40.72°N and 80.15°E – 80.53°E. This area was characterized by an extreme continental arid desert climate with annual average values of precipitation and evaporation as 40.1 – 82.5 mm and 1,876.6 – 2,558.9 mm, respectively. The annual sunshine hours ranged from 2,556.3 to 2,991.8 h. According to the meteorological data from the local weather station, the lowest temperature of -15 to -24℃ was recorded in January, while the highest temperature of 33 to 39℃ was recorded in July or August with an annual mean value of 10.7℃. Benefiting from the freshwater sources provided by the local government, cotton, jujube, and other perennial plants were cultivated here as the main economic plants. Soil was moistened by mulched drip irrigation, and seasonal flood irrigation occurred every spring and winter to leach accumulated salt.

Soil sample collection and determination

In the oasis within the headstream area of the Tarim River, Xinjiang, China, 106 sites with longitude and latitude recorded were selected for study in October 2019, including 76 sites in the cotton field and 30 sites in the jujube orchard. A 0 – 200 cm soil profile was evenly divided into 10 layers with an individual layer thickness of 20 cm. At every site, ten replicate samples from the same depth were mixed homogenously, and a quarter of the soil was packaged in a sterile polyethylene plastic bag and brought back to laboratory. A total of 1,060 soil samples were air dried uniformly, and the visible stones, roots, and debris were removed before being manually ground and finally passed through a 20-mesh sieve. 40 g air-dried soil was mixed with deionized water at a ratio of 1:5 and homogenized at 180 rpm for 1 h using Kylin-Bell QB-328 end-over-end shaker (Haimen Kylin-Bell Lab Instruments Co., Ltd., Haimen, Jiangsu, China). The mixture was centrifuged at 4,500 rpm for 5 minutes, and the supernatant was passed through 0.45 µm filters [18]. An aliquot of 1 mL 0.1 M $Al_2(SO_4)_3$ and 10 mL filtrates were diluted to 50 mL before the soluble K^+ and Na^+ were determined by using FP6410 flame photometer (Shanghai Xinyi Precision Instrument Co., Ltd., Shanghai, China). After correcting by the dilution factor, the soil soluble K^+ and Na^+ contents were obtained. Soil soluble Ca^{2+}, Mg^{2+}, and SO_4^{2-} were determined by mixing a 10 mL aliquot of the filtrate with diluted ammonium chloride–ammonia buffer solution (pH 10) and K-B indicator followed by titration with 0.01 M EDTA standard solution. Soil Cl^- content was determined by adding potassium chromate indicator to the filtrate and titrating with 0.025 M silver nitrate standard solution. Soil CO_3^{2-} and

HCO_3^- contents were measured by titrating the filtrate with 0.01 M H_2SO_4 standard solution. Phenolphthalein indicator was then added followed by dropwise addition of bromophenol blue indicator [19]. Soil total dissolved salt (TDS) content was calculated as the sum of eight salt ions described above. Predominant nutrient indices included available P, K, and mineral N. Soil available P was measured by extracting air-dried soil with 0.5 M $NaHCO_3$. After adding molybdenum antimony resistance reagent to the filtered filtrate, the absorbance was measured by using PERSEE T500 UV-Vis spectrophotometer (Beijing Puxi General Instrument Co., Ltd., Beijing, China). Soil available K in the filtered filtrate was determined by extracting air-dried soil with 1 M NH_4OAc followed by using a flame photometer [19]. Mineral N was composed of nitrate and ammonium N and was extracted by 1 M KCl followed by using SEAL Analytical AA3 continuous flow analyzer (SEAL Analytical Instruments (Shanghai) Co., Ltd., Shanghai, China) [20].

Statistical analysis

All experiments were performed in duplicate. The results were expressed as mean ± standard deviation (SD). The correlation between soil salt ions and their contribution to TDS was explored by principal component analysis (PCA). Kaiser-Meyer-Olkin (KMO) statistics (> 0.5) and Bartlett's test (< 0.05) were conducted to confirm the adequacy of PCA. Linear correlation analysis and significance test were achieved by using SPSS 26.0 (IBM, Armonk, NY, USA). Data figures were plotted by using Origin 2016 (https://www.originlab.com/).

Predictive model construction

To elucidate the relationship between salt or nutrient content across different layers within the 0 – 200 cm soil profile, this study employed data from all 106 profiles to establish a universal predictive model that captured the general patterns governing the vertical distribution of soil salinity or nutrient indicators within the study area. Global models were constructed 9 times with every layer being used as a variable once to serve two purposes of predicting deeper layers and predicting the entire profile. Individual optimization was pursued. While global models reflected overall average trends, each profile possessed unique characteristics. The global models were applied to each independent profile, calculating prediction errors for different models. The layer number (p) corresponding to the model yielding the minimum prediction error was identified as the critical layer for predicting the layer of that profile. Similarly, q was identified as the decisive layer for predicting the entire profile. The predictive analysis of salt content was based on only TDS, while nutrient contents were separated as available P, available K, and mineral N, respectively. The random forest (RF) model implemented in Python 3.5 (https://www.python.org/) was selected as the core analytical tool, which was an ensemble learning algorithm that predicted by constructing and combining a large number of decision trees and was particularly adept at handling complex, multi-dimensional data [21]. The randomness of RF was reflected in two aspects including the randomness of feature selection and data sampling. Together, these two sources of randomness gave each decision tree unique characteristics, effectively avoiding overfitting and making the model's predictions accurate and stable. 80% of the total samples were randomly selected with replacement to construct the regression tree, while the remaining 20% samples were used as out-of-bag data to evaluate the model performance and the importance of independent variables. The final prediction results of the regression tree were obtained by voting or taking the average value. Then, the predicted value and the measured value of the validation set were compared. Prediction accuracy of different methods was evaluated by calculating the mean square error (MSE), root mean square error (RMSE), mean absolute error (MAE), mean absolute percentage error (MAPE), and coefficient of determination (R^2) of the validation set as follows.

$$MSE=\frac{1}{N}\sum_{i=1}^{N}\left(y_i-\bar{y}_i\right)^2 \tag{1}$$

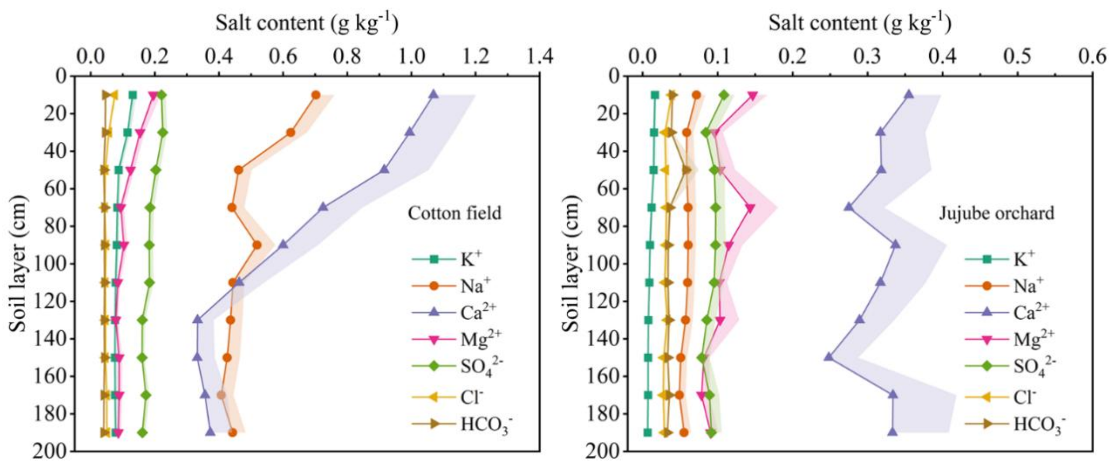

Figure 1. Contents of salt along soil 0 – 200 cm profile of cotton field and jujube orchard.

$$\mathrm{RMSE}=\sqrt{\frac{1}{N}\sum_{i=1}^{N}\left(y_i-\bar{y}_i\right)^2} \quad (2)$$

$$\mathrm{MAE}=\frac{1}{N}\sum_{i=1}^{N}\left|y_i-\bar{y}_i\right| \quad (3)$$

$$\mathrm{MAPE}=\frac{1}{N}\sum_{i=1}^{N}\left|\frac{y_i-\bar{y}_i}{y_i}\right|\times 100\% \quad (4)$$

$$R^2=1-\frac{\sum_{i=1}^{N}\left(y_i-\bar{y}_i\right)^2}{\sum_{i=1}^{N}\left(\bar{y}_i-\hat{y}_i\right)^2} \quad (5)$$

where N was the number of soil samples. $\bar{y}_i$ was the measured value of salt or nutrient content. $\hat{y}_i$ was the average of the measured value. y_i was the predictive value of each model. Lower values of MSE, RMSE, MAE, and MAPE indicated higher accuracy, while an R^2 value closer to 1 indicated a better fit [22].

Results and discussion

Characteristics of salt content during 0 – 200 cm profile

The proportion of Ca^{2+} was the highest among all detected salt ions, ranging from 38.92 – 48.02%, and the ratio of $Cl^-/2SO_4^{2-}$ was less than 0.20 in most samples. According to the local classification standards for salinized soil in Xinjiang, China [23], the tested samples were classified as calcium-sulfate type slightly salinized soil. Seven salt ions were quantified and no CO_3^{2-} was detected in the soil samples from either location. The contents of Ca^{2+} and Na^+ were higher than other salt ions with the means of 1.07 and 0.70 g/kg in the 0 – 20 cm layer, respectively, which decreased as the soil depth increased until hitting a plateau of 0.3 – 0.5 g/kg during 120 – 140 cm. SO_4^{2-} content averaged 0.19 g/kg and showed a non-significant difference between layers. Trace Mg^{2+}, K^+, and Cl^- were only detected in the topsoil. Meanwhile, the HCO_3^- was extremely low during the whole profile. However, their proportion in TDS rose gradually. In the case of the jujube orchard, Ca^{2+} similarly accounted for the highest content during 0 – 200 cm profile, ranging from 0.09 – 2.18 g/kg and 0.31 g/kg, respectively. It exhibited a slight decrease in 60 – 80 cm and 120 – 160 cm intervals but remained comparable to surface levels in deeper soil. Conversely, Mg^{2+} showed relatively higher content in these two layers, indicating that Mg^{2+} was possible main competing ion for Ca^{2+} in jujube orchard soil. The content of SO_4^{2-} was close to Mg^{2+} followed by Na^+, Cl^-, and HCO_3^-, which either decreased or remained stable with depth. The TDS contents ranged from 1.17 to 2.43 g/kg and 0.53 to 0.78 g/kg for cotton fields and jujube orchards, respectively, with up to 51.3% of salts distributed in the top 40 cm and deeper layers (Figure 1). Generally, the TDS content in cotton field was higher than that in jujube orchard, and the difference was mainly

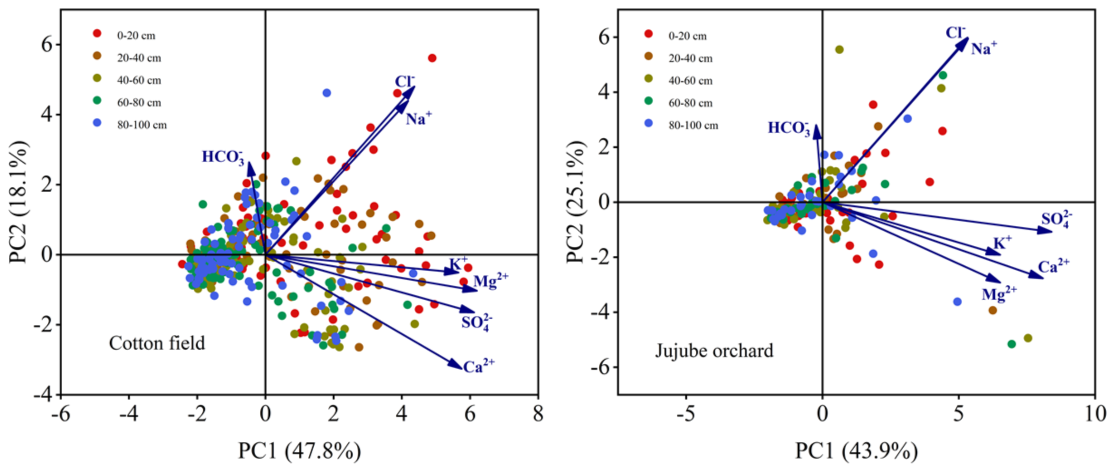

Figure 2. Principal component analysis of salt ions (K^+, Na^+, Ca^{2+}, Mg^{2+}, SO_4^{2-}, Cl^-, HCO_3^-) in 0 – 100 cm soil collected from cotton field and jujube orchard.

due to Ca^{2+} and Na^+, which possibly attributed to the reasons that farmland was generally reclaimed from silt-clay soil, which had a stronger ability to retain nutrients. By contrast, orchards were cultivated by leveling sandy soil. There was a noticeable correlation between soil texture and salt content as the higher proportion of clay particles, the stronger water-holding capacity, and the more salt accumulation [24, 25]. Additionally, drip irrigation technology was applied in cotton fields from 2004, whereas flooding irrigation remained common among jujube orchards. Salt was leached towards deep underground during flooding irrigation [26, 27]. The decrease in TDS content with the increase of soil depth was more notable in the cotton field. Simultaneously, less irrigation and great evaporation led to the salt accumulation in the upper soil surface. To explore the correlation of various salt ions, principal component analysis was conducted. In terms of 0 – 100 cm soil in the cotton field, the first and second PCA respectively explained 47.8% and 18.1% of the total variance among all parameters, which accounted for 43.9% and 25.1% to jujube orchard. All seven detected salt ions were divided into 3 parts including that HCO_3^- was independent, Na^+ and Cl^- were almost identical and they might come from same source or have similar mobile capacity, Ca^{2+}, Mg^{2+}, SO_4^{2-} and K^+ were clustered along the PC1, showing significant positive correlation, likely due to fertilization with Ca^{2+}, Mg^{2+}, SO_4^{2-}, K^+ in cotton field and jujube orchard demonstrating 0.432, 0.465, 0.459, 0.424 and 0.485, 0.391, 0.504, 0.391, all showing the higher component loading on PC1, indicated that they mainly drove the variation of TDS content during 0 – 100 cm soils (Figure 2).

Characteristics of nutrients during 0 – 200 cm profile

The N, P, and K contents were key indices for assessing the levels of soil fertility. The results showed that the mineral N, available P, and K contents were decreased with the increasing of soil depth in both areas. The content of available K was the highest in the cotton field with the mean values from 64.89 mg/kg in 200 cm underground to 107.86 mg/kg in surface soil. Mineral N and available P also reached their highest levels in 0 – 20 cm as 68.23 mg/kg and 31.21 mg/kg, respectively. However, in 180 – 200 cm soil layer, they declined to 21.91 and 1.25 mg/kg, respectively. Similar decrease trend was observed in jujube orchard, where mineral N, available P, and K were 32.1 – 81.59, 3.78 – 64.76, and 64.27 – 125.77 mg/kg, respectively. Most available nutrients concentrated in 0 – 40 cm topsoil, which was a zone of active root and microorganism and secreted acid and enzymes to decompose insoluble nutrients to meet growth requirements [28]. Plant demand for P was

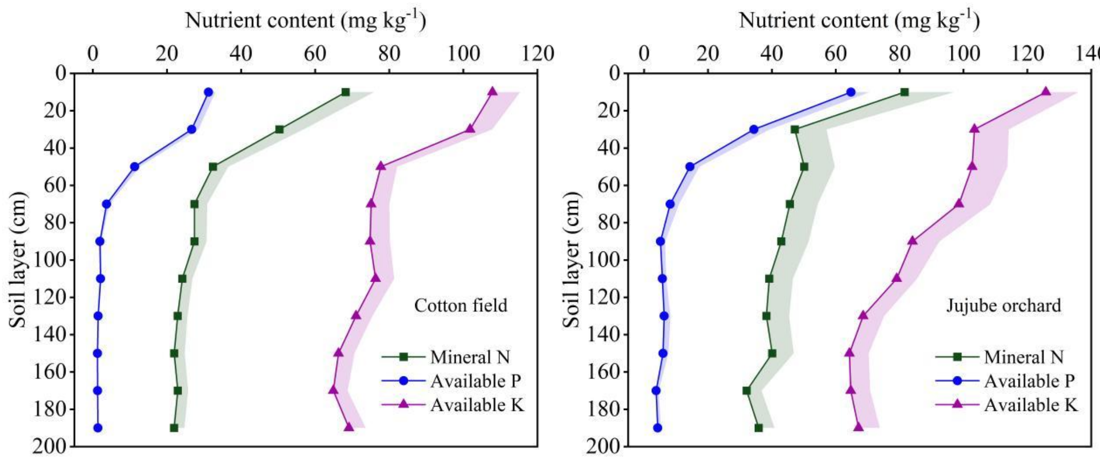

Figure 3. Contents of nutrient along soil 0 – 200 cm profile of cotton field and jujube orchard.

relatively low compared with N and K. The application rate of P fertilizer was correspondingly low [29]. But more importantly, the mobility of P was restrained in saline-alkali soil and readily combined with Ca^{2+} and Mg^{2+} to form insoluble minerals, which were difficult to extract by $NaHCO_3$ solution [30]. Reportedly, the migration range of P in the soil was limited within a few centimeters [31]. Hence, available P was extremely low below the 40 cm soil. Nevertheless, mineral N and available K exhibited stronger mobility and decreased *via* irrigation. As root density decreased, as well as nutrient uptake reduced, labile N and K accumulated in the deeper layer [32]. Overall, these three nutrient contents were higher in the jujube orchard than that in the cotton field, which was related to various fertilizer application rates according to crop types. In general, more fertilizer was applied to the orchard than to the field due to the higher nutrient requirement from bigger biomass. Therefore, higher nutrient accumulation was observed in the orchard [33]. Additionally, jujube is a potassium-loving plant. Producers tend to invest more K fertilizer than in a cotton field, and its roots can penetrate more than 1.0 m into the ground to absorb nutrients. Therefore, the available K content in orchard soil decreased at a uniform rate with depth and was lower than that in the cotton field when the soil depth was deeper than 100 cm (Figure 3).

Correlations between salt and nutrient contents

The correlation analysis between TDS and three nutrient indices was conducted in the main arable layer (0 – 100 cm). The results showed that mineral N in the cotton field exhibited a positive correlation from 0 – 100 cm. The coefficient of determination R^2 was 0.311 in the 0 – 20 cm layer and reduced with increasing soil depth (Figure 4). The available K similarly showed positive correlation, but no clear trend with depth was observed (Figure 5). On the contrary, the correlation between available P and TDS was not significant in any soil layer (Figure 6). The mineral N only showed significant correlation in the range of 0 –20 cm in the jujube orchard, while no significant correlation was observed between available K and available P across the entire 0 – 100 cm profile. The results indicated that there was a correlation between salt and nutrients. The correlation was stronger for mineral N and available K than available P, and it was stronger in the top layer than in the deep layer. Generally, salt entered to soil *via* applying mineral fertilizer, and their distribution characteristics rely on element mobility properties and moisture fluctuation. The N and K elements were more labile in soil than P, their mobility behavior was the closest to free salt ions, which were readily transported by irrigation and evaporation [34]. Consequently, they were found alongside salt ions, especially in the topsoil where fertilizer and

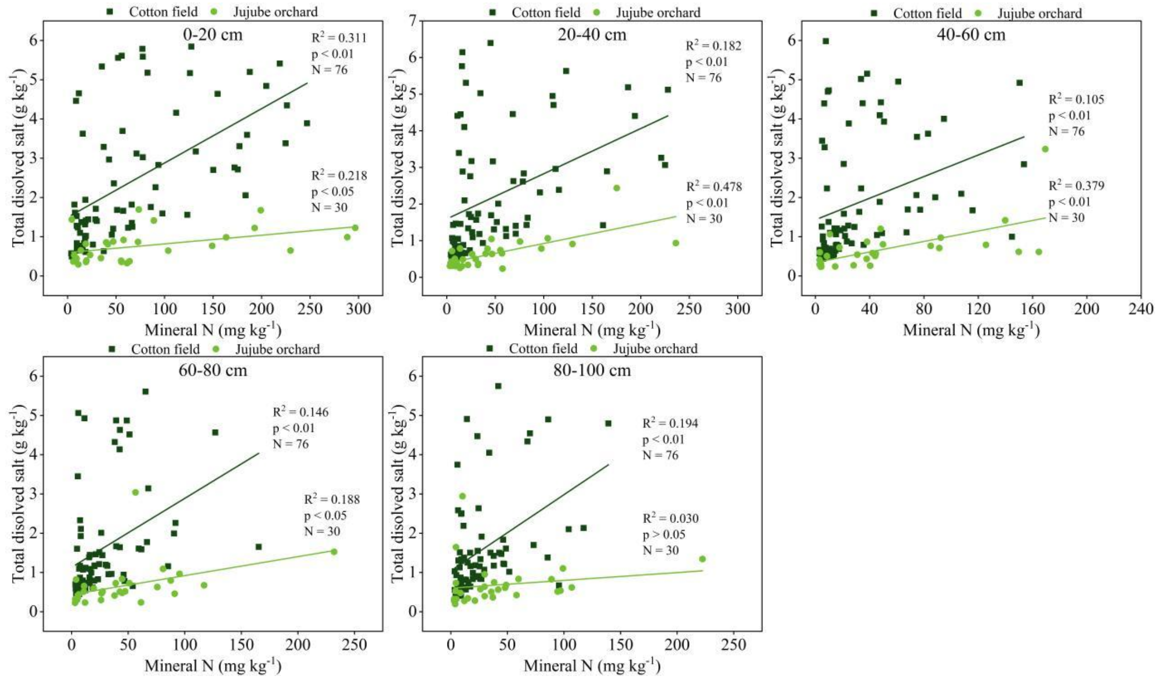

Figure 4. The correlation between the total dissolved salt and mineral N during 0 – 100 cm.

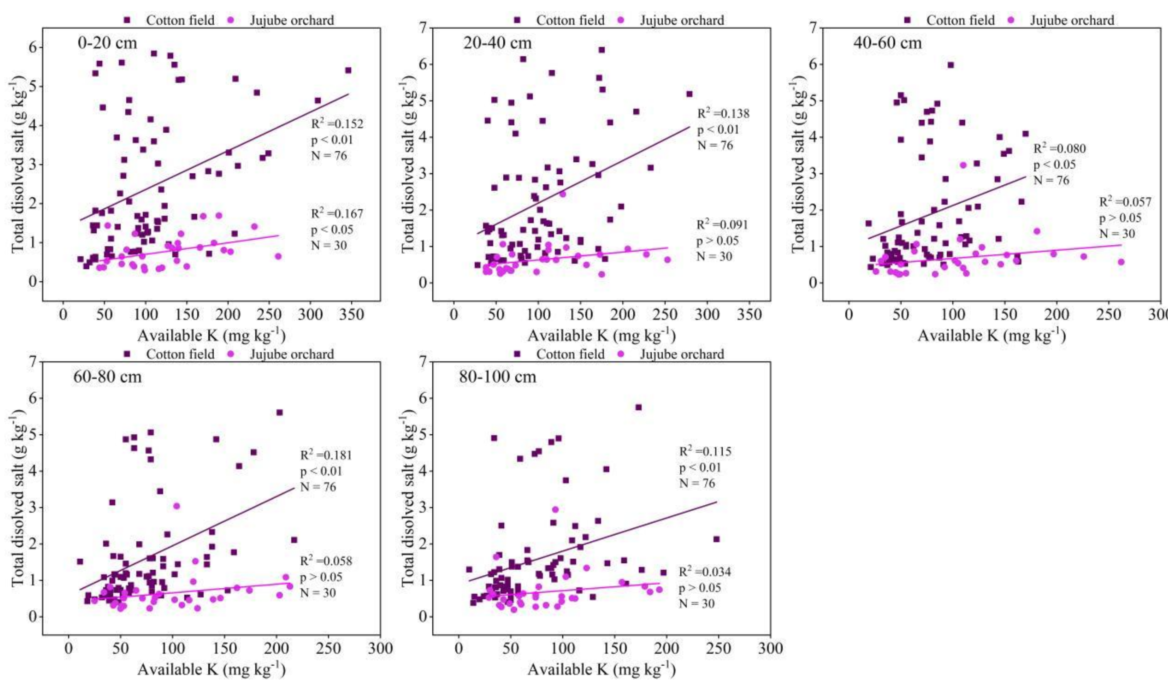

Figure 5. The correlation between the total dissolved salt and available K during 0 – 100 cm.

water were often accumulated. Relatively, P is immobilized rapidly after application and remains near the application point and seldom moves to a wider area. This explains why P always shows a non-significant correlation with salt in both present and previous research [35].

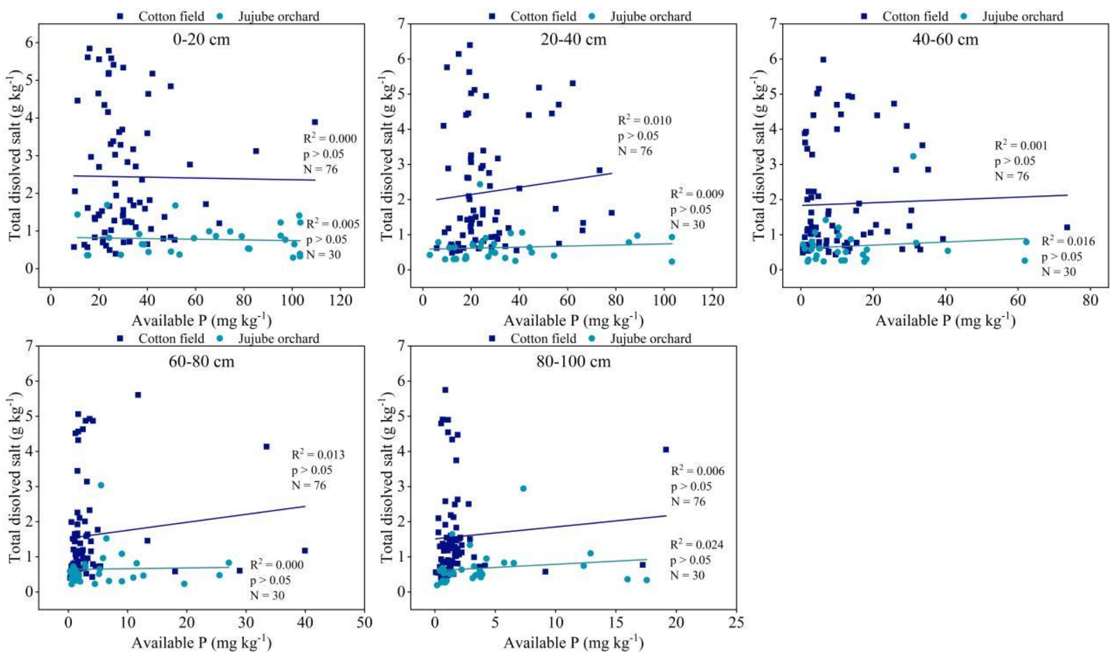

Figure 6. The correlation between the total dissolved salt and available P during 0 – 100 cm.

Predictive modeling of soil salinity and nutrients

Traditional research requires collecting actual samples and conducting measurements to understand the salt content or nutrient levels in the soil. However, this is inconvenient for deeper soil layers because drilling or excavating profiles is time-consuming and labor-intensive. Given the need for the South Xinjiang farmland to understand the conditions of the deep soil layers, the random forest model was used to explore whether measuring partial upper soil salt and nutrient data could accurately predict the contents of the deeper layers and the entire profile. In this study, each 20 cm section on the profile was considered as one layer. Assuming there was a layer n, the total TDS sum from the surface to layer p ($\sum_{i=1}^{p} TDS$) was correlated with the $\sum_{i=p+1}^{10} TDS$ from layer p + 1 to the bottommost layer (180 – 200 cm), and the layer with the highest R^2 among the 106 p layers was selected as the critical layer with predictive capabilities for the deeper layers. Similarly, a layer q could be inferred, that is, the $\sum_{i=1}^{q} TDS$ could better predict the data of the entire profile. The performance of the global model ensured the accuracy of individual optimization. The coefficient of determination R^2 was used to evaluate the fit of each model. The R^2 values of all models were very high from 0.83 to 0.92 for cotton field and 0.92 to 0.99 for jujube orchard, proving that there was a close intrinsic relationship between the TDS of the upper soil and the TDS of the deeper layers and the entire profile. The values of MSE, RMSE, MAE, and MAPE were less than 6.23, 2.49, 1.76, and 17.56, respectively, indicating high accuracy of the models. The p-series models for predicting the lower layers demonstrated a performance peak of 0.9226 at p = 2, meaning that using the data from 40 cm of the surface (layers 1 and 2) to predict the TDS of the lower 160 cm (layers 3 to 10) was the most effective. In the q-series models for predicting the entire profile, the R^2 value steadily increased with q and approached 1, where the R^2 value was as high as 0.9604. The R^2 value was already as high as q = 2 at sampling depth of 40 cm, demonstrating strong predictive ability. These findings suggested that the upper 40 cm of soil might represent a critical salt activity layer with its cumulative information serving as the strongest indicator of salinization status in deeper soil layers. The same model was applied to nutrient prediction. For N, P, and K, the prediction showed a better result in the jujube orchard with higher R^2 than it in the cotton field. The R^2 values for the p-series models predicting mineral N and available K in the lower layers were less than 0.9 along with relatively high error indices such as MAE, indicating low model accuracy. Although the q-series models for predicting the entire profile exhibited higher R^2 values, their precision remained concerning. The model for available P exhibited a higher R^2 and smaller error. Theoretically, a critical layer might exist between 80 and 100 cm. However, due to the low mobility of P, there was a weak correlation between deep-layer available P and surface layers. Furthermore, the results showed that the available P content in the 60 – 100 cm soil layer dropped below 5 mg/kg (Figure 3). Thus, the predictive results held limited practical significance. These findings indicated that predicting deeper or full-profile data based on surface data was more applicable for salts than nutrients. In practice, the primary factor influencing salt distribution was soil moisture. During flood irrigation, it exhibited a “regular triangle” pattern from shallow to deep layers, whereas evaporation produced an “inverted triangle” distribution [14]. Therefore, strong correlations existed between soil salinity levels across different layers, which also explained the low correlation coefficients between nutrients and salinity observed in this study. Plant growth showed minimal impact on areas with high-concentration salinity, but it significantly influenced the distribution of low-concentration nutrients. Moreover, inconsistent nutrient demand among plants and varying root uptake efficiency across soil layers can weaken the correlation of nutrients between adjacent layers such as deeper taproots often absorb less than shallow lateral roots [36]. Overall, the random forest model was suitable for predicting deep-layer salt content. Measuring salt content at 20 – 40 cm generally indicated the salinization level of deeper layers or the entire profile (0 – 200 cm). This approach could eliminate the need to excavate the deepest soil layers for determination.

Conclusion

This study revealed distinct soil salinity and nutrient stratification in the oasis agricultural area within the headstream area of the Tarim River, Xinjiang, China, challenging conventional assumptions about salt-nutrient coupling. The results showed that soil salinity concentrations ranged from 1.17 to 2.43 g/kg and 0.53 to 0.78 g/kg for cotton fields and jujube orchards, respectively, with up to 51.3% of salts distributed in the top 40 cm. Salinity levels were primarily driven by four ions of Ca^{2+}, Mg^{2+}, SO_4^{2-}, and K^+, which exhibited strong correlations and were jointly introduced through fertilization. However, salinity-nutrient correlations were surprisingly ion-specific, confined to mineral N and available K in topsoil. A key finding indicated that the 20 – 40 cm soil layer could serve as a "sentinel" depth for salinity monitoring, thereby enabling a rapid and labor-efficient assessment of the entire soil profile without the need for exhaustive sampling. These findings bridged methodological pragmatism with scientific rigor and underscored that dual impacts of fertilization on salinity and nutrients remained surface-bound with root uptake governing vertical nutrient distribution rather than leaching. These patterns diverged markedly between cotton and jujube systems, reflecting cultivation-specific legacies of each cultivation system. Collectively, this work advanced precision agriculture in arid reclaimed lands by identifying actionable depth targets and clarifying how agronomic practices reshaped soil chemical architecture.

Acknowledgements

This work was funded by the open fund of Observation and Research Station of Soil and Water Process and Ecological Security of Oasis in the Headstream Area of the Tarim River, MNR (Grant No. 2025BSYK-06) and the President’s Fund of Tarim University (Grant No. TDZKBS202503).

References

1. Feng Q, Yin XW, Zhu M, Zhang JT, Liu W, Xi HY, *et al*. 2024. Overall promotion of integrated management and utilization of saline-alkali land in Northwest China: Conditions, challenges, and recommendations. Bull Chin Acad Sci. 39(12):2060-2073.
2. Wang XF, Wang YJ, Zhou XF, Zhao X, Xu H. 2024. Analysis of soil changes and carbon sequestration potential in saline areas of Xinjiang. Coal Geol China. 36(5):55-55 + 75.
3. Saifullah, Dahlawi S, Naeem A, Rengel Z, Naidu R. 2018. Biochar application for the remediation of salt-affected soils: Challenges and opportunities. Sci Total Environ. 625:320-335.
4. Wang YS, Cui Y, Su H, Jiang JX, Wang Y, Yang ZL, *et al*. 2022. Response of calcareous nannoplankton to the Paleocene-Eocene Thermal Maximum in the Paratethys Seaway (Tarim Basin, West China). Global and Planet Change. 217:103918.
5. Chen Y, Zhang JZ, Wang ZH, Li HQ, Chen R, Zhao Y, *et al*. 2024. Influence of long-term mulched drip irrigation on upward capillary water movement characteristics in the saline-sodic region of northwest China. Agronomy. 14(6):1300.
6. Dai JL, Cui ZP, Zhang YJ, Zhan LJ, Nie JJ, Cui JQ, *et al*. 2024. Enhancing stand establishment and yield formation of cotton with multiple drip irrigation during emergence in saline fields of Southern Xinjiang. Field Crops Res. 315:109482.
7. Hui R, Tan HJ, Li XR, Wang BY. 2022. Variation of soil physical-chemical characteristics in salt-affected soil in the Qarhan Salt Lake, Qaidam Basin. J Arid Land. 14(3):341-355.
8. Liu YF, Yang QW, Pei XJ, Li JJ, Wang SC, Huang ZF, *et al*. 2024. Spatial distribution of soil salinization under the influence of human activities in arid areas, China. J Arid Land. 16(10):1344-1364.
9. Ye YS, Wang HY, Zhang PP, Zhang YH. 2025. Adaptation strategies for hemp in alkaline salt environments: Fertilizer management for nutrient uptake and optimizing growth. Agriculture. 15(2):125.
10. Chen JS, Gao Y, Wang XP, Wang GS. 2022. Seasonal variation in water uptake depth of jujube estimated with stable isotopes: Comparative study of drip and basin irrigation. J Soil Sci Plant Nutr. 22(1):443-454.
11. Zhang W, Wang BJ, Gan YW, Duan ZP, Hao XD, Xu WL, *et al*. 2019. Competitive interaction in jujube tree/cotton agroforestry system in Xinjiang province, northwestern China. Agrofor Syst. 93(2):591-605.
12. Qian YZ, Zhu Y, Ye M, Huang JS, Wu JW. 2021. Experiment and numerical simulation for designing layout parameters of subsurface drainage pipes in arid agricultural areas. Agric Water Manage. 243:106455.
13. Genedi MA, Ahmed MA. 2024. Salinity distribution in agricultural land by geophysical, hydrochemical and geostatistical approaches: a pilot area located in Qelabshowah-Belqas, East Nile Delta region, Egypt. Environ Earth Sci. 83(9):269.
14. Guan ZL, Jia ZF, Zhao ZQ, You QY. 2019. Dynamics and distribution of soil salinity under long-term mulched drip irrigation in an arid area of northwestern China. Water. 11(6):1225.
15. Dou CY, Lv YP, Sun YD, Chen XP, Li Y. 2024. Assessment of soil nutrients in plant root layer of a saline-sodic soil cropped with *Lycium barbarum* L. when drip irrigated with saline groundwater. Agronomy. 14(7):1374.
16. Sothe C, Gonsamo A, Arabian J, Snider J. 2022. Large scale mapping of soil organic carbon concentration with 3D machine learning and satellite observations. Geoderma. 405:115402.
17. Zhang HR, Fu X, Zhang YN, Qi ZS, Zhang HC, Xu ZH. 2023. Mapping multi-depth soil salinity using remote sensing-enabled machine learning in the Yellow River Delta, China. Remote Sens. 15(24):5640.
18. Setia R, Rengasamy P, Marschner P. 2013. Effect of exchangeable cation concentration on sorption and desorption of dissolved organic carbon in saline soils. Sci Total Environ. 465:226-232.
19. Handbook of soil analysis: Mineralogical, organic and inorganic methods. Edited by Pansu M. Berlin, Heidelberg: Springer Berlin Heidelberg; 2006.
20. Liu Y, Li ZY, Deng KY, Zhou Q, Xu RK. 2017. Effect of nitrogen forms on reduction of manganese oxides in an Oxisol by plant root exudates. Arch Agron Soil Sci. 63(12):1725-1735.
21. Breiman L. 2001. Random forests. Mach Learn. 45(1):5-32.
22. Zheng MW, Wen QQ, Xu FY, Wu DS. 2025. Regional forest carbon stock estimation based on multi-source data and machine learning algorithms. Forests. 16(3):420.
23. Xinjiang Agricultural Technology Manual. Edited by Xinjiang Academy of Agricultural Sciences. Urumqi, Xinjiang: Xinjiang People's Publishing House; 1976.
24. Wang ZM, Li GM, Li X, Shan S, Zhang JY, Li SY, *et al*. 2012. Characteristics of moisture and salinity of soil in Taklimakan Desert, China. Water Sci Technol. 66(6):1162-1170.
25. Wen D, Wang JJ, Ding JL, Zhang Z. 2025. Distribution characteristics and relationship between soil salinity and soil particle size in Ebinur lake wetland, Xinjiang. Land. 14(2):297.
26. Liu ZP, Jiao XY, Lu SH, Zhu CL, Zhai YM, Guo WH. 2019. Effects of winter irrigation on soil salinity and jujube growth in arid regions. Plos One. 14(6):e0218622.
27. Ren JW, Guo TK, Tian CY, Mai WX, Mao XM. 2025. Modeling water and salt migration in groundwater and vadose zones to assess agricultural sustainability in Karamay Irrigation District. Agric Water Manage. 317:109611.
28. Wang JG, Tian T, Wang HJ, Cui J, Shi XY, Song JH, *et al*. 2022. Chitosan-coated compound fertilizer application and crop rotation alleviate continuous cotton cropping obstacles by modulating root exudates. Rhizosphere. 23:100581.
29. Yibati H, Zhang Y, Li QJ, Xu XP, He P. 2022. Estimation of cotton nutrient uptake based on the QUEFTS model in Xinjiang. Agronomy. 12(6):1427.
30. Shi YXX, Yu YC, Chang E, Wang RH, Hong ZN, Cui JQ, *et al*. 2023. Effect of biochar incorporation on phosphorus supplementation and availability in soil: A review. J Soils Sediments. 23(2):672-686.
31. Stecker JA, Brown JR, Kitchen NR. 2001. Residual phosphorus distribution and sorption in starter fertilizer bands applied in no-till culture. Soil Sci Soc Am J. 65(4):1173-1183.
32. Zhang Y, Wu LG, Zhang X, Deng AX, Abdulkareem R, Wang DZ, *et al*. 2022. Effect of long-term organic amendment application

on the vertical distribution of nutrients in a vertisol. Agronomy. 12(5):1162.

33. Huang XR, Gao HB, Chen K, Wang CX, Gao PC. 2025. Land-use change from wheat fields to kiwifruit orchards increases fluoride accumulation and associated environmental risks. J Hazard Mater. 496:139520.
34. Palanivell P, Ahmed OH, Latifah O, Majid NMA. 2020. Adsorption and desorption of nitrogen, phosphorus, potassium, and soil buffering capacity following application of chicken litter biochar to an acid soil. Appl Sci. 10(1):295.
35. Chen BL, Sheng JD, Dai TT, Liu YG. 2012. Preliminary research on the correlation between soil phosphorus and salt ions in cotton field. J Xinjiang Agric Univ. 35(03):222-226.
36. James M, Masclaux-Daubresse C, Balliau T, Marmagne A, Chardon F, Trouverie J, *et al*. 2024. Multi-scale phenotyping of senescence-related changes in roots of rapeseed in response to nitrate limitation. J Exp Bot. 76(2):312-330.